Electronic Quasiparticle Renormalization on the Spin Wave Energy Scale

J. Schäfer,[1] D. Schrupp,[1] Eli Rotenberg,[2] K. Rossnagel,[2] H. Koh,[2] P. Blaha,[3] and R. Claessen[1]

[1]*Institut für Physik, Universität Augsburg, 86135 Augsburg, Germany*

[2]*Advanced Light Source, Lawrence Berkeley National Laboratory, Berkeley, California 94720, USA*

[3]*Institut für Materialchemie, Technische Universität Wien, A-1060 Wien, Austria*

(Received 8 October 2003; published 4 March 2004)

High-resolution photoemission data of the (110) iron surface reveal the existence of well-defined metallic surface resonances in good correspondence to band calculations. Close to the Fermi level, their dispersion and momentum broadening display anomalies characteristic of quasiparticle renormalization due to coupling to bosonic excitations. Its energy scale exceeds that of phonons by far, and is in striking coincidence with that of the spin wave spectrum in iron. The self-energy behavior thus gives spectroscopic evidence of a quasiparticle mass enhancement due to electron-magnon coupling.

DOI: 10.1103/PhysRevLett.92.097205 PACS numbers: 75.30.Ds, 73.20.At, 75.50.Bb, 79.60.–i

The electronic properties of metals are determined by the dynamical behavior of the conduction electrons. Conventional band theory accounts for their interaction with the static ion lattice, yet coupling to further microscopic degrees of freedom can alter the electron dynamics. Low energy electrons (or holes) become dressed by a cloud of virtual excitations, thereby forming *quasiparticles* of increased effective mass and reduced Fermi velocity. Beyond a characteristic energy scale ω_0, determined by the spectrum of the coupled excitations, the electrons lose their dressing and resume their noncoupling band dispersion. A prominent example is the interaction with phonons [1]. Quasiparticle formation due to electron-phonon coupling has recently been studied in great detail by angle-resolved photoelectron spectroscopy (ARPES) [2–4]. In contrast, the effect of coupling to other bosonic excitation modes, notably spin excitations in magnetic materials, is not well established. This problem has received new attention due to the suggestion that high-temperature superconductivity in cuprate materials may result from electronic coupling to spin fluctuations [5,6]. Unfortunately, similar energy scales of phonon and spin excitations are a serious hindrance for determining relative interaction strengths in the cuprates [7–9].

A prime candidate to explore the interaction of electrons with spin waves is ferromagnetic iron. Here the energy scale of the spin waves [10,11] is approximately an order of magnitude higher than that of the phonons. Furthermore, the recent observation of superconductivity in the nonmagnetic high-pressure phase of Fe [12] has been related to electronic coupling with spin fluctuations [13]. A detailed analysis of quasiparticle renormalization and related electronic self-energy effects is best achieved by ARPES on surface states [4,14]. Previous ARPES studies of Fe, particularly of the Fe(110) surface [15,16], have, however, been inconclusive regarding the existence of metallic surface states due to a rather limited resolution.

In this Letter, we report on high-resolution angle-resolved photoemission of the Fe(110) surface. Two metallic surface state bands are identified which display spectroscopic signatures of quasiparticle renormalization. The analysis of real and imaginary parts of the self-energy extracted from the data yield a characteristic energy scale of $\sim$160 meV, much larger than the phonon energy scale yet in good correspondence to the magnon spectrum of Fe. We thus interpret these data as direct spectroscopic evidence of electronic renormalization effects in a magnetic solid due to coupling with spin wave excitations.

Experimentally, samples of very high surface purity were generated by evaporating thick bcc iron films *in situ* onto a W(110) substrate. Annealing at 500 °C ensures a well-ordered surface seen in electron diffraction. ARPES was performed at $T = 85$ K at beam line 7.0.1 of the Advanced Light Source in Berkeley. A Scienta SES-100 electron analyzer was used with a momentum resolution of $\sim$0.012 Å^{-1} and a total energy resolution of $\sim$35 meV.

The analysis of ARPES data in terms of single-particle excitation spectra and self-energy effects requires the localization of the probed electronic states perpendicular to the surface, as satisfied by surface states and resonances [14]. For ferromagnetic iron, the (110) surface provides such states with the required metallic character. For identifying location and spin orientation, we have performed a 23-layer density functional theory calculation [17]. Metallic surface states exist around the $\bar{\mathrm{N}}$ and around the $\bar{\mathrm{S}}$ points of the Brillouin zone and are of spin-down (*minority*) character. Here we focus on the surface bands $\mathbf{s}_1$ and $\mathbf{s}_2$ whose energy dispersion is shown in Fig. 1. Concerning possible spin interaction, they overlap in energy with the surface-projected bulk bands of opposite spin, thereby enabling spin-flip scattering processes between surface and bulk states. A full account of surface band structure and Fermi surface topology will be published elsewhere.

In the following, we will concentrate on the experimental dispersion of these surface states near the Fermi

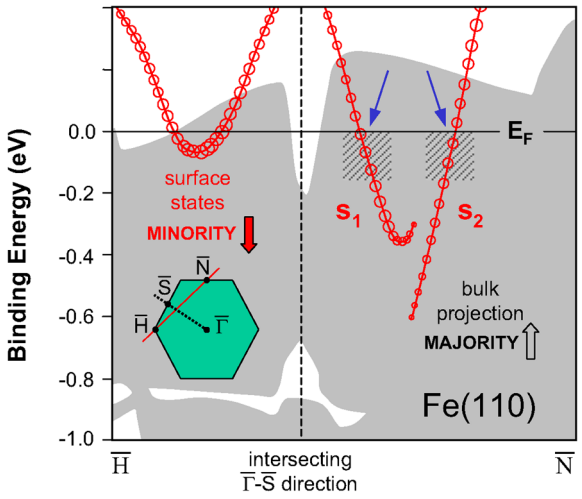

FIG. 1 (color online). Band structure of the (110) surface of ferromagnetic iron, calculated by density functional theory (inset: surface Brillouin zone). The two metallic surface resonances $\mathbf{s}_1$ and $\mathbf{s}_2$ are used for line shape analysis (surface character indicated by circle size). The gray-shaded area represents the surface-projected bulk band structure of opposite spin.

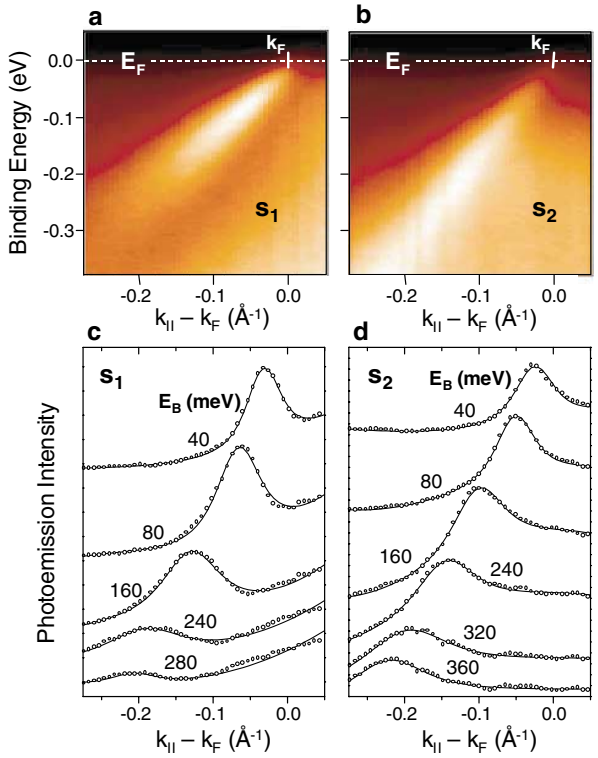

FIG. 2 (color online). ARPES raw data of the surface states $\mathbf{s}_1$ and $\mathbf{s}_2$ near the Fermi level. (a) Intensity map of the $\mathbf{s}_1$ band ($h\nu = 110$ eV) with high intensity in the quasiparticle region. (b) Band map of $\mathbf{s}_2$ ($h\nu = 112$ eV). (c) Spectra in k direction of the $\mathbf{s}_1$ state which can be fitted well with a Lorentzian-Gaussian peak model (indicated). (d) Spectra of the $\mathbf{s}_2$ state.

level. For highest intensity, data were recorded along the $\bar{\Gamma} - \bar{\mathrm{S}}$ direction for $\mathbf{s}_1$, and along $\bar{\mathrm{H}} - \bar{\mathrm{N}}$ for $\mathbf{s}_2$. In the raw data of surface state $\mathbf{s}_1$ in Fig. 2(a), the dressed quasiparticle shows up with comparatively high intensity, extending beyond 0.1 eV binding energy. State $\mathbf{s}_2$ extends to rather high binding energies on a gradually increasing background, as shown in Fig. 2(b).

The accurate peak position and width is obtained from a fit [4] of the momentum distribution curves (MDCs) at constant energy shown in Figs. 2(c) and 2(d). We employed a convoluted Lorentzian-Gaussian line shape and a polynomial background. Here the Gaussian part takes care of the experimental broadening, while the Lorentzian width component is used for the self-energy analysis. While with such fit analysis peak positions can be determined to an accuracy better than the experimental broadening, uncertainty arises from a weak peak asymmetry and the varying baseline which leads to a systematic error of ± 0.004 Å^{-1} for the position and $\pm 10\%$ for the width of the peak.

The dispersions based on the peak positions of both surface states $\mathbf{s}_1$ and $\mathbf{s}_2$ are compiled in Figs. 3(a) and 3(b), respectively. Both dispersions display a weak "kink" in the 100–200 meV region below E_F, which phenomenologically is very similar to quasiparticle renormalization effects observed for electron-phonon coupling [2–4]. The dispersion anomaly is particularly obvious when comparing the actual dispersion to the nominally "undressed" band. The latter is obtained by parabolic interpolation between the lowest data points and the experimental Fermi vector. The experimentally determined dispersion is significantly offset from the smooth noncoupling band interpolation. A dispersion anomaly is not found in the band structure calculation of Fig. 1. The interpolation, however, is in reasonable agreement with the calculation regarding the occupied bandwidth. Therefore one is led to conclude that the observed kinks are indeed caused by many-body effects beyond the bare band picture.

Deviations from noninteracting behavior of the electrons can be described in terms of the electronic self-energy Σ as a function of binding energy [14]. The real part $\mathrm{Re}\,\Sigma(\omega)$ is the difference between interpolated and observed band dispersion, as plotted in Fig. 4(a). For both surface bands, it increases towards a maximum around 125 ± 10 meV and then gradually approaches zero again. The imaginary part of the self-energy, $\mathrm{Im}\,\Sigma(\omega)$, reflects scattering processes for which the available phase space increases with increasing binding energy. It is given by the Lorentzian half-width of the MDC (converted to an energy scale using the undressed band slope). Impurity scattering [4] adds a small offset of ~ 30 meV. The results for $\mathrm{Im}\,\Sigma(\omega)$ after offset subtraction are displayed in Fig. 4(b). A pronounced increase of $\mathrm{Im}\,\Sigma(\omega)$ with binding energy saturates at $\sim 160 \pm 20$ meV. The two self-energy components are very much the same for both surface states concerning spectral shape and magnitude, thus

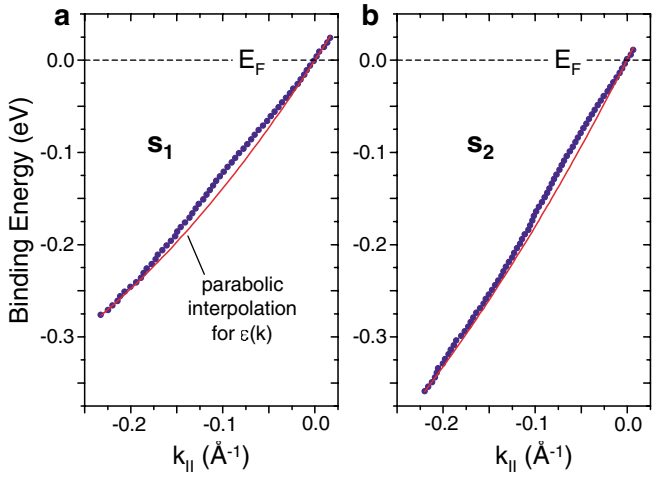

FIG. 3 (color online). (a) Dispersion for $\mathbf{s}_1$ obtained from fitting the spectra (thick dots). The noninteracting band $\varepsilon(k)$ is interpolated by a parabola between the lowest binding energy data and the E_F crossing (smooth line). The difference between thick dots and smooth line curves is ascribed to renormalization. (b) Same for the $\mathbf{s}_2$ state.

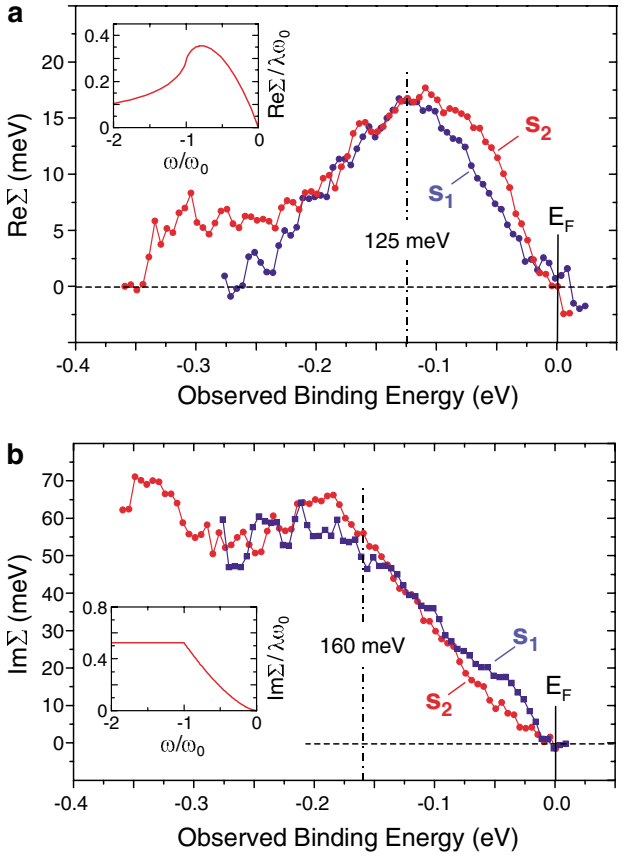

FIG. 4 (color online). Experimental self-energies of states $\mathbf{s}_1$ and $\mathbf{s}_2$. (a) Real part Re Σ as the difference between observed and interpolated dispersion. The inset shows Re Σ from a spin wave model in units of ω_0 with a maximum at $0.79\omega_0$ (see text for details). (b) Imaginary part Im Σ derived from the width of the MDCs. A plateau is observed at $\omega_0 \sim 160 \pm 20$ meV. Im Σ from the spin wave model is shown in the inset.

pointing to a common origin. Note that Im $\Sigma(\omega)$ determined in this way also contains the contribution of spin-independent electron-electron scattering, which is expected to be smoothly increasing with energy over the entire bandwidth. In contrast, Re $\Sigma(\omega)$ as displayed in Fig. 4(a) does not contain electron-electron interaction effects, as they are already absorbed within the undressed band interpolation.

Concerning possible mechanisms responsible for the observed self-energy effects, the large energy scale of $\sim$160 meV clearly rules out electron-phonon coupling as origin. The phonon spectrum of iron has a maximum energy of $\sim$30 meV in the bulk [18] and also at the (110) surface [19]. While it may affect the spectral behavior there, it cannot be considered relevant on a larger binding energy scale. Electron-electron scattering through Coulomb interaction is another source of self-energy effects [4]. Since in iron the total electronic density of states is smooth in the relevant energy region, such contributions cannot account for characteristic structure in the spectra. Thus, we are left to consider coupling of the electrons with magnetic excitations as a source of the effect.

Spin waves (*magnons*) in ferromagnetic Fe are well known from inelastic neutron scattering [10,11,20]. Between approximately 100 and 200 meV, both experiment [11] and theory [21,22] find an "acoustic" and an "optical" magnon branch, separated by a gap where sharply defined spin waves do not exist. An acoustic spin wave branch has also been inferred from the temperature dependence of the magnetization, locating its cutoff at 166 meV [23]. This energy scale is remarkably close to the characteristic energy of the observed ARPES anomalies. It suggests their interpretation in terms of electron-magnon coupling-induced quasiparticle renormalization, assuming that the electrons couple predominantly to the acoustic spin waves and only weakly to the optical modes.

Independent evidence comes from spin-polarized electron energy loss spectroscopy (SPEELS) on the Fe(110) surface [24,25]. A loss structure at 170–200 meV is interpreted as exchange scattering by spin waves, in very good agreement with our ARPES data. We also note that a very recent SPEELS study on ultrathin Co films observed strong electronic interaction only with the acoustic (surface) magnon branch, but no obvious signs of the additional optical modes [26].

The compatibility of the ARPES self-energies with an electron-magnon coupling scenario can be tested using a simple model in analogy to electron-phonon coupling. There, in the most simple picture Im Σ can be written as integral over the phonon density of states ρ_{ph}:

$$\mathrm{Im}\,\Sigma(\omega) \propto \lambda \int_0^{\omega} \rho_{\mathrm{ph}}(\Omega)\, d\Omega,$$

where λ is a dimensionless coupling constant [1]. For a spin wave mechanism ρ_{ph} has to be replaced by the magnon density of states $\rho_{\mathrm{mag}}(\omega) \propto \omega^{1/2}$ if the quadratic magnon dispersion in ferromagnets is considered. Assuming coupling only to the acoustic spin wave branch, ρ_{mag} is cut off at its maximum energy ω_0. For the case of coupling to bulk spin waves, this yields $\mathrm{Im}\,\Sigma(\omega) \propto \omega^{3/2}$ for $\omega < \omega_0$ and constant behavior above the cutoff energy. $\mathrm{Re}\,\Sigma(\omega)$ is obtained from a Kramers-Kronig relation and exhibits a maximum at $0.79\omega_0$, beyond which it decays asymptotically. The resulting self-energy components are displayed in the insets of Figs. 4(a) and 4(b).

Comparing the model to our self-energy data, best agreement is achieved for a cutoff energy of $\omega_0 = 160 \pm 20$ meV. This choice reproduces the peak of $\mathrm{Re}\,\Sigma$ at $\sim$125 meV. For $\mathrm{Im}\,\Sigma$, ω_0 accurately marks the onset of the plateau in the data, while the magnitude of the experimental $\mathrm{Im}\,\Sigma$ exceeds the model as expected from the additional contribution of electron-electron scattering (not contained in the $\mathrm{Re}\,\Sigma$ data, as mentioned above). Our crude spin wave model thus gives a surprisingly good description of the functional form of the data. This extends the analysis beyond the comparison of energies and is additional evidence for spin wave dressing of the electrons.

The strength of the electron-spin wave scattering is described by the coupling constant λ. It is given by the prefactor of $\mathrm{Re}\,\Sigma$, or equivalently by the Fermi velocity which is renormalized by $1/(1 + \lambda)$. Both definitions yield an experimental value of $\lambda = 0.20 \pm 0.04$, indicating a relatively small coupling strength. It may be contrasted with mass enhancement factors between $\lambda = 0.5$ and 2 from de Haas–van Alphen experiments on bulk Fe [27] (note that the origin of this renormalization was not resolved in that paper). The moderate coupling observed here may be traced back to two effects: (i) the available phase space for spin-flip scattering between spin-down and spin-up surface states in a ferromagnet is expected to be reduced if the exchange splitting between them is considerably larger than the magnon energy scale; (ii) here the scattering occurs from spin-down *surface* states into spin-up *bulk* states, however the small spatial overlap of surface and bulk states will limit the effective scattering strength.

For *antiferromagnetic* metals (or nonmagnetic metals near a magnetic instability), such phase space limitations do not exist and much stronger coupling strengths are to be expected. Notably, this also holds for the superconducting cuprates which are close to an antiferromagnetic ground state and display pronounced spin fluctuations [28]. The phenomenology of the quasiparticle renormalization will qualitatively be the same as for the ferromagnetic case, with details depending on the precise shape of the magnetic excitation spectrum [29]. Our observations therefore provide spectroscopic evidence that the renormalization effects seen by ARPES in the cuprates [7,9] are also highly compatible with strong coupling to magnetic fluctuations, an important prerequisite for models of high-temperature superconductivity based on spin-mediated pairing [5,6].

The authors are grateful to M. Hochstrasser for the electron beam evaporator and M. Hoinkis for technical support. Discussion of the spin wave model with P. Riseborough is gratefully acknowledged. This work was supported by the DFG (Grant No. CL 124/3-2 and SFB 484), and by the BaCaTeC program.

[1] G. Grimvall, *The Electron-Phonon Interaction in Metals* (North-Holland, Amsterdam, 1981).
[2] M. Hengsberger *et al.*, Phys. Rev. Lett. **83**, 592 (1999).
[3] E. Rotenberg, J. Schäfer, and S. D. Kevan, Phys. Rev. Lett. **84**, 2925 (2000).
[4] T. Valla *et al.*, Phys. Rev. Lett. **83**, 2085 (1999).
[5] P. Monthoux and D. Pines, Phys. Rev. Lett. **69**, 961 (1992).
[6] K. Ueda *et al.*, J. Phys. Chem. Solids **53**, 1515 (1992).
[7] M. Eschrig and M. R. Norman, Phys. Rev. Lett. **85**, 3261 (2000).
[8] A. Lanzara *et al.*, Nature (London) **412**, 510 (2001).
[9] E. Schachinger *et al.*, Phys. Rev. B **67**, 214508 (2003).
[10] H. A. Mook and R. M. Nicklow, Phys. Rev. B **7**, 336 (1973).
[11] D. McKenzie Paul *et al.*, Phys. Rev. B **38**, 580 (1988).
[12] K. Shimizu *et al.*, Nature (London) **412**, 316 (2001).
[13] T. Jarlborg, Physica (Amsterdam) **385C**, 513 (2003).
[14] *Angle-Resolved Photoemission*, edited by S. D. Kevan (Elsevier, Amsterdam, 1992).
[15] H.-J. Kim *et al.*, Surf. Sci. **478**, 193 (2001).
[16] E. Vescovo *et al.*, Phys. Rev. B **48**, 285 (1993).
[17] P. Blaha, K. Schwarz, G. K. H. Madsen, D. Kvasnicka, and J. Luitz, computer code WIEN2K—an augmented plane wave plus local orbitals program (Vienna, 2001).
[18] A. Dal Corso and S. Gironcoli, Phys. Rev. B **62**, 273 (2000).
[19] G. Benedek *et al.*, Phys. Rev. Lett. **68**, 2644 (1992).
[20] C.-K. Loong *et al.*, J. Appl. Phys. **55**, 1895 (1984).
[21] K. Karlsson and F. Aryasetiawan, Phys. Rev. B **62**, 3006 (2000).
[22] J. A. Blackman *et al.*, Phys. Rev. Lett. **55**, 2814 (1985).
[23] J. C. Ododo and M. W. Anyakoha, J. Phys. F **13**, 2335 (1983).
[24] M. Plihal *et al.*, Phys. Rev. Lett. **82**, 2579 (1999).
[25] M. R. Vernoy, H. Hopster, and D. L. Mills, AVS 49th International Symposium (MI-WeA5, 2002).
[26] R. Vollmer *et al.*, Phys. Rev. Lett. **91**, 147201 (2003).
[27] G. G. Lonzarich, J. Magn. Magn. Mater. **45**, 43 (1984).
[28] J. P. Carbotte *et al.*, Nature (London) **401,** 354 (1999).
[29] D. Manske *et al.*, Phys. Rev. B **67**, 134520 (2003).